Journal Pre-proof

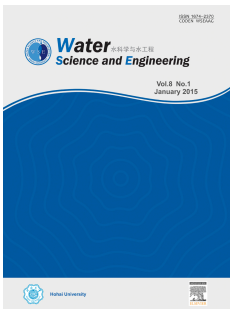

Degradation of tetracycline in water using hydrogen peroxide activated by soybean residue-derived magnetic biochar

Van-Truc Nguyen, Duy-Dat Nguyen, Thi-Giang-Huong Duong, Viet-Cuong Dinh, Thi-Dieu-Hien Vo

PII: S1674-2370(24)00100-5

DOI: https://doi.org/10.1016/j.wse.2024.10.001

Reference: WSE 421

To appear in: *Water Science and Engineering*

Received Date: 20 May 2024

Accepted Date: 27 September 2024

Please cite this article as: Nguyen, V.-T., Nguyen, D.-D., Duong, T.-G.-H., Dinh, V.-C., Vo, T.-D.-H., Degradation of tetracycline in water using hydrogen peroxide activated by soybean residue-derived magnetic biochar, *Water Science and Engineering*, https://doi.org/10.1016/j.wse.2024.10.001.

Degradation of tetracycline in water using hydrogen peroxide activated by soybean residue-derived magnetic biochar

Van-Truc Nguyen [a], Duy-Dat Nguyen [b], Thi-Giang-Huong Duong [a], Viet-Cuong Dinh [c], Thi-Dieu-Hien Vo [d, *]

[a] *Faculty of Environment, Saigon University, Ho Chi Minh City 700000, Vietnam*

[b] *Faculty of Chemical & Food Technology, Ho Chi Minh City University of Technology and Education, Ho Chi Minh City 700000, Vietnam*

[c] *Faculty of Environmental Engineering, Hanoi University of Civil Engineering, Hanoi 100000, Vietnam*

[d] *Institute of Applied Technology and Sustainable Development, Nguyen Tat Thanh University, Ho Chi Minh City 700000, Vietnam*

Received 20 May 2024; accepted 27 September 2024
Available online

Abstract

Tetracyclines (TCs) are the second most commonly used antibiotics worldwide, utilized both in medical treatments and animal husbandry. Although effective against various infectious diseases, TC residues persist in the environment and contribute to the emergence of antibiotic-resistant pathogens, posing significant risks to human health. This study employed the heterogeneous Fenton process to degrade TC using soybean residue-derived magnetic biochar (Fe-SoyB) as the catalyst. The Fe-SoyB sample was characterized using X-ray diffraction (XRD), scanning electron microscopy (SEM), Fourier-transform infrared spectroscopy (FTIR), and superconducting quantum interference device (SQUID) techniques. The effects of key parameters, including pH, H_2O_2 concentration, catalyst dosage, and initial TC concentration, on TC degradation were investigated. The results indicated that the TC removal efficiency decreased with increasing initial TC concentration, while it was improved with higher H_2O_2 concentrations and greater catalyst dosages. The optimal conditions for the Fenton-like process were determined to a pH of 3, a H_2O_2 concentration of 245 mmol/L, an initial TC concentration of 800 mg/L, and a catalyst dosage of 0.75 g/L, achieving a removal efficiency of 90% after 150 min. Additionally, the TC removal efficiency of the Fe-SoyB system varied significantly across different water matrices, with 87.1% for deionized water, 78.5% for tap water, and 72.5% for river water. The catalyst demonstrated notable stability, maintaining a TC removal efficiency of 79.7% after three cycles of use. Overall, Fe-SoyB shows promise as a cost-effective catalyst for the elimination of organic pollutants in aqueous solutions.

Keywords: Catalyst; Magnetic biochar; H_2O_2;Tetracycline; Fenton-like process

1. Introduction

Biochar is a carbon-rich material produced from various biomass sources, including plants, food waste, and animal waste, through pyrolysis (Fu et al., 2019; Wijitkosum, 2022; Zhao et al., 2023). It is emerging as a versatile material with numerous applications, such as energy production, soil quality enhancement, heavy metal removal, catalysis, and fuel cell applications (Ganesapillai et al., 2023). Biochar synthesized from agricultural waste biomass is highly valued due to the increasing need for innovative environmental management solutions within the circular economy framework. The global scientific community's interest in biochar stems from its potential to address environmental issues, such as improving soil quality and purifying polluted water environments. As a soil conditioner and adsorbent, biochar offers significant opportunities within the circular economy model. With the ongoing energy transition, applications of low-emission materials will drive progress towards net-zero emissions. Literature suggests that converting biomass into biochar supports the achievement of the United Nations Sustainable Development Goals (Kurniawan et al., 2023). While the implementation of sustainable technologies for environmental issues often faces high investment costs, biochar production through the pyrolysis of waste biomass presents an economically and environmentally variable (Li et al., 2023).

Literature indicates that biochar can be produced from a diverse range of biomass sources, including agricultural residues, fruit peels, micro- and macro-algae, sawdust, wood, and wastewater sludge (Son et al., 2018; Santhosh et al., 2020). Soybean residues have been identified as a potentially suitable source for biochar production due to its low cost and widespread availability. According to latest forecast from the United States Department of Agriculture, global soybean production in the 2023/2024 crop year is expected to increase by 8.9% compared to the 2022/2023 crop year, rising from 369.7×10^6 t to 402.8×10^6 t (USDA, 2024). Soybean residues are generated in large quantities during the production of oil, milk, bean curd, and tofu from soybeans. Approximately 87.17% of soybean residues are produced during the cold pressing process (Mateos-Aparicio et al., 2010). They are considered a low-cost source of dry matter, with a protein content of about 46.8%, and are often used as a source of plant protein food. However, on a nutritional basis, soybean residues are less valuable than both corn and wheat residues. Despite this, soybean residues can utilized as a feedstock

*Corresponding author.
E-mail address: vtdhien@ntt.edu.vn (Thi-Dieu-Hien Vo)

for biofuel and chemical production. Given their cellulose content of about 6.8% and the large quantities generated annually, utilizing soybean residues as a raw material for the production of functional carbon materials, such as biochar, is highly beneficial.

In the past five years, numerous studies have focused on the application of biochar for water. Antibiotic pollution has become a major concern due to the overuse of these substances in both human medicine and veterinary practices. Antibiotics persist in the environment and pose significant risks to human and animal health, even at trace levels (Liu et al., 2015). Tetracycline (TC), the second most widely used antibiotic, has been extensively employed in livestock feed and disease control for several decades (Nikzad et al., 2024). The presence of tetracycline (TC) residues in the environment has facilitated the development and spread of TC-resistant genes, further endangering human and animal health (Zhu et al., 2013). Therefore, it is necessary to find effective technologies for removing TC from contaminated aqueous environments (Ortiz-Ramos et al., 2022; Zhao et al., 2024).

Biochar used to remove TC is produced from various waste biomass sources, including rice husks (Luo et al., 2023), sunflower seed husks (Nguyen et al., 2023), kitchen waste (Sun et al., 2023a), banana peels (Zhang et al., 2023b), cotton stems (Qin et al., 2023), Suaeda seepweeds (Jiang et al., 2023), poplar wood (Zhang et al., 2023a), wheat straw (Huang et al., 2023), sugarcane bagasse (Tang et al., 2023), crayfish shell (Jiang and Dai, 2023), cornstalks (Sun et al., 2023b), walnut shells (Shi et al., 2023), and sludge (Hu et al., 2023). Studies have shown that biochar is effective in removing antibiotics in water, particularly TC. Biochar derived from soybean residues contains a high carbon content, ranging from 37.4% to 44.8%, depending on the pyrolysis temperature. In addition, soybean residue-based biochar contains functional groups (e.g., =C–H, –C–H, C=O, and C=C) that are suitable for adsorption processes (Sun et al., 2021). A recent study by Li et al. (2021) used soybean residues to synthesize biochar for the adsorption of TC hydrochloride with the aid of a peroxydisulfate activator, achieving an 84% removal rate of TC. However, the performance of biochar does not yet match that of traditional activated carbon. Therefore, ongoing research efforts aim to enhance the pollutant removal performance of biochar (Du et al., 2023; Zhang et al., 2024).

Fe-modified materials, such as Fe^0, FeS, and Fe_3O_4, have garnered significant attention in recent years due to their enhanced treatment efficiency (Lee et al., 2023; Peng et al., 2023). Goethite (α-FeOOH), a natural, low-cost, and widely available mineral, is widely used to remove contaminants from water. However, its activity can decrease due to agglomeration. Biochar serves as an excellent support material for transition metals (such as Fe, Co, and Ni), which helps mitigate agglomeration and enhances pollutant degradation efficiency. Combining metal oxyhydroxide and carbon catalysts to activate hydrogen peroxide (H_2O_2) is highly feasible. Advanced oxidation processes (AOPs) have proven highly effective in degrading persistent organic pollutants by generating highly reactive free radicals that oxidize organic contaminants (Ghanbari et al., 2020). Among AOPs, Fenton and Fenton-like oxidation, which utilize catalysts such as Fe^{2+}/Fe^{3+} and H_2O_2, are particularly efficient techniques for the degradation and mineralization of organic contaminants in wastewater (Nidheesh, 2015; Kakavandi and Babaei, 2016). In advanced oxidation, the reaction of catalysts with H_2O_2 forms strong oxidizing radicals (·OH with an oxidation potential of 2.80 V), promoting the decomposition of organic matter (Su et al., 2018, 2022).

Previous studies have investigated H_2O_2 activation with an α-FeOOH/biochar mixture for removing organic pollutants (Chen et al., 2023; Huang et al., 2023) and heavy metals (Isaac et al., 2023; Yang et al., 2024). However, literature shows that there are no detailed studies on soybean residue-derived biochar modified with goethite to activate H_2O_2 for the removal of TC in aqueous solutions. Therefore, this study applied biochar derived from soybean residues modified with goethite activated H_2O_2 for TC removal in aqueous solutions. The morphological and structural properties of the biochar were analyzed to evaluate its adsorption potential. Factors such as pH, H_2O_2 concentration, initial TC concentration, and biochar dosage were meticulously studied. TC removal capacity in different water environments and biochar recycle studies were conducted, and the underlying mechanisms were also proposed.

2. Materials and methods

2.1. Chemicals

Tetracycline hydrochloride ($C_{22}H_{24}N_2O_8$·HCl with a molecular weight of 480.90 g/mol and a purity greater than 99.0%) was purchased from Sigma Aldrich. All other reagents, including potassium hydroxide (KOH with a purity of 99%), hydrochloric acid solution (HCl with a concentration of 37%), hydrogen peroxide (H_2O_2 with a purity of 30%), and ferric chloride ($FeCl_3.6H_2O$ with a

*Corresponding author.
E-mail address: vtdhien@ntt.edu.vn (Thi-Dieu-Hien Vo)

purity of 97%), were obtained from Xilong Chemical Co., Ltd., China. All chemicals were analytically pure and were directly utilized in the experiments without any additional treatment or purification. Solutions were prepared with deionized (DI) water.

2.2. Synthesis of biochar (Fe-SoyB)

Soybean residues were collected from traditional markets in Ho Chi Minh City, Vietnam. The residues were thoroughly washed with DI water and then dried at 105℃ in an oven (DK-500 DT, Yihder Technology Co., Ltd., Taiwan, China) for 24 h. The dried residues were sieved to obtain a particle size of approximately 0.25 mm for use in this study. To prepare soybean biochar (SoyB), the dried soybean residues were calcinated in a furnace at 500℃ for 2 h, with a heating rate of 10℃ per minute and an N_2 purging flow rate of 100 mL/min (Cho et al., 2017; Nguyen et al., 2021). The resulting SoyB material was stored in an air-tight container for subsequent activation steps. 1.0 g of SoyB was mixed with KOH at a KOH-to-SoyB weight ratio of 4:1 in 10 mL of DI water in a stainless-steel cup using a magnetic mixer for 2 h. The mixture was then dried at 140℃ for 4 h. The stainless-steel cup containing the mixture was then sealed and calcinated in an air-tight furnace at 800℃ for 2 h, with a N_2 purging flow rate of 100 mL/min (Li et al., 2017). The resulting biochar was denoted as KOH-SoyB. Goethite (α-FeOOH) was synthesized from $FeCl_3$. Briefly, 50 mL of 1-mol/L $FeCl_3{\cdot}6H_2O$ and 90 mL of 5-mol/L KOH were vigorously mixed using a magnetic stirrer, with a small amount of DI water added initially. Additional DI water was then added to bring the final volume to 1 000 mL. The synthesizing process for the Fe composite material followed the steps for goethite generation but with a minor change. KOH-SoyB was initially added to the $FeCl_3{\cdot}6H_2O$ and KOH mixture at a weight ratio of 2:1. The mixture was then calcinated in an airtight furnace at 500℃ for 2 h, with a N_2 purging flow rate of 100 mL/min. After pyrolyzing, the resulting soybean-activated carbon loaded with goethite was referred to as Fe-SoyB.

2.3. TC degradation experiments

To evaluate the catalytic efficiency of the Fe-SoyB catalyst, the TC solution was chosen as the target pollutant. The degradation experiments used the Fe-SoyB catalyst at a dose of 0.50 g/L, H_2O_2 at a concentration of 245 mmol/L, and TC at a concentration of 800 mg/L. The experiments were performed in 50-mL conical tubes mounted on a digital rotator (MX-RD Pro, DRAGON Lab., China) and rotated at a speed of 100 r/min at room temperature. The Fenton-like reaction was initiated by adding a known amount of H_2O_2 to the solution. At predetermined time intervals, 7.0 mL of samples were withdrawn and filtered using 0.22-μm syringe filter discs to remove suspended particles. The obtained filtrate was measured by ultraviolet–visible (UV–vis) spectrophotometers (Halo XB-10 and VIS-20, Dynamica Scientific Ltd., the United Kingdom) at a wavelength of 357 nm (Weidner et al., 2021). To investigate the effect of pH on TC degradation, experiments were conducted at different pH values (3.0, 5.0, 7.0, and 9.0). In addition, the effects of varying H_2O_2 concentrations (223–490 mmol/L), TC concentrations (600–1 000 mg/L), and Fe-SoyB dosages (0.25–0.75 g/L) were studied. All experiments were performed in triplicate. Under optimal conditions (ρ(Fe-SoyB) = 0.75 g/L, ρ(TC) = 800 mg/L, c(H_2O_2) = 245 mmol/L, and a reaction time of 150 min), cycling experiments of TC degradation were conducted using the Fe-SoyB-activated H_2O_2 system to investigate the stability of Fe-SoyB. After each experiment, the TC concentration was measured. Without any regeneration treatment, Fe-SoyB was recycled for subsequent experiments by centrifugation at 5 000 r/min for 5 min. The stability of Fe-SoyB was determined by computing the TC removal efficiency computed at the end of each round.

River water samples were collected from the Sai Gon River, Vietnam, between 9:00 AM and 11:00 AM (local time, GMT +7). The collection and preservation of water samples followed the standard methods for the examination of water and wastewater (Baird et al., 2017). To avoid surface scum, samples were taken from a depth of 20–30 cm below the river's surface. Three 2-L samples were obtained: two from near the riverbanks and one from the river center. These samples were combined in a 10-L container, mixed thoroughly, and then transferred into 2-L polyethylene terephthalate (PET) bottles for laboratory analysis. The samples were kept on ice during transport to the laboratory. The characteristics of the Sai Gon River water, used to investigate TC degradation in the water matrix, were as follows: pH of 7.11, temperature ranging from 29.0°C to 30.5°C, chemical oxygen demand (COD) of 106 mg/L, total suspended solids (TSS) of 300 mg/L, turbidity of 75 nephelometric turbidity units (NTU). The experimental procedure was the same as previously mentioned. Additionally, electron paramagnetic resonance (EPR) analysis was conducted using a Bruker EMX-10

*Corresponding author.
E-mail address: vtdhien@ntt.edu.vn (Thi-Dieu-Hien Vo)

spectrometer (Karlsruhe, Germany) with an X-band frequency of 9.49–9.88 GHz and a power of 8.02 mW. 5,5-dimethylpyrroline-oxide (DMPO) was employed as a spin-trapping agent to identify the active radicals produced by H_2O_2 activation.

2.4. Analytical methods

The surface morphologies of the materials and the main surface elements were analyzed using scanning electron microscopy (SEM) images and energy dispersive X-ray spectroscopy (EDS) data (JSM-6510 LV), respectively. The magnetic properties of the catalysts were investigated using a superconducting quantum interference device magnetometer (MPMS-XL7, Quantum Design, San Diego, California, USA). Fourier-transform infrared spectroscopy (FTIR; FT/IR-4600) was employed to identify the main functional groups on the surface of the biochar. The biochar particles were pelleted using KBr before analysis. The infrared (IR) spectrum was obtained by co-adding 20 scans at a resolution of 2 cm^{-1} over a range of 400–4 000 cm^{-1}. The crystalline phases in the synthesized materials were identified using X-ray diffraction (XRD) patterns (D6 Advance Bruker, equipped with Cu Kα radiation at a wavelength of 0.154 06 nm) with a germanium detector for 2θ (where θ is the diffraction angle) values of 0°–70° at a scan rate of 0.03° per minute. The point of zero charge (pH_{PZC}) of Fe-SoyB was determined using the method described by Jang and Kan (2019) and Nguyen et al. (2021). The pH_{PZC} value of Fe-SoyB was indicated by adjusting the initial pH (pH_{Before}) of 100-mL NaCl solutions ranging from 3.0 ± 0.1 to 10.0 ± 0.1 using 0.1 mol/L of HCl or NaOH, followed by the addition of 0.02 g of Fe-SoyB. The mixtures were shaken for 8 h at 25°C and then separated using filter papers to measure the final pH (pH_{After}). The pH_{PZC} value of Fe-SoyB was estimated by plotting pH_{Before} against ΔpH ($\Delta pH = pH_{After} - pH_{Before}$). In this study, the TC concentration was determined using UV–vis spectrophotometers (Halo XB-10 and VIS-20, Dynamica Scientific Ltd., the United Kingdom) at a wavelength of 357 nm.

2.5. Data statistical methods

All experiments were performed in triplicate. The data obtained from the study were processed and statistically analyzed using IBM SPSS Statistics version 25, Microsoft Excel 2010, and OriginPro (OriginLab Corporation).

3. Results and discussion

3.1. Characterization of Fe-SoyB

The SEM image (Fig. 1(a)) illustrated the morphology of Fe-SoyB, revealing a heterogeneous and rough surface with slight protrusions. This surface morphology is advantageous for adsorption, as it can provide more adsorption sites for binding adsorbates (Akindolie and Choi, 2022; Zhang et al., 2024). The energy dispersive X-ray spectroscopy (EDX) data of Fe-SoyB (Fig. 1(b)) confirmed high percentages of carbon (approximately 65%) and oxygen (approximately 20%) on the surface of the biochar, with iron present at around 11%. This indicated successful incorporation of Fe into SoyB. The FTIR technology was utilized to identify the functional groups present in the Fe-SoyB material. As shown in Fig. 1(c), the FTIR spectrum exhibited a band at 3 387 cm^{-1}, indicating O–H stretching (Zhu et al., 2014; Liu et al., 2020). The presence of oxygen-containing functional groups on Fe-SoyB, such as carboxyl and hydroxyl groups, enhanced TC adsorption through hydrogen bonding (Sun et al., 2012; Wang et al., 2017). Additional peaks were assigned as follows: (1) a peak at 2 853 cm^{-1} associated with C–H bonds, representing the stretching vibration of aliphatic hydrocarbons (Sevilla and Fuertes, 2009; Nguyen et al., 2019b); (2) peaks at 1 009 cm^{-1}, 1 085 cm^{-1}, and 1 196 cm^{-1} corresponding to C=O and C–O–C groups (Jaiswal et al., 2021); (3) peaks at 633 cm^{-1} and 512 cm^{-1} related to C–C stretching groups (Jaiswal et al., 2021); (4) a peak at approximately 476 cm^{-1} representing the stretching vibration of the Fe–O functional group (Devi and Saroha, 2017). Fig. 1(d) shows the magnetic properties of Fe-SoyB. A magnetization saturation value of 43.2 $A{\cdot}m^2/kg$ was observed for Fe-SoyB. This strong magnetic responsivity suggested that Fe-SoyB was easily attracted to external magnets and removed from the system after the reaction (Li et al., 2022b). XRD analysis was performed to assess the crystallinity of the catalysts. The XRD patterns of Fe-SoyB exhibited peaks at 2θ values of 14.9°, 15.5°, 17.4°, 24.3°, 28.9°, 29.0°, 30.1°, 31.2°, 35.2°, 39.3°, 45.8°, 49.9°, and 60.1° (Fig. 1(e)). As noted by Jaiswal et al. (2013) and Markovski et al. (2014), peaks at 2θ values of 24.3°, 35.2°, 39.3°, 49.9°, and 60.1° are characteristic of goethite. These XRD patterns, consistent with SEM and EDX results, indicated that Fe was effectively loaded

*Corresponding author.
E-mail address: vtdhien@ntt.edu.vn (Thi-Dieu-Hien Vo)

onto the biochar surface. Additionally, the crystallite size of Fe-SoyB was calculated using the Scherer equation (Massoudi et al., 2020):

$$D = \frac{K\lambda}{\beta \cos\theta} \quad (1)$$

where D is the crystallite size, K is the shape factor (K = 0.94), β is the full width at half maximum of the peak, and λ is the wavelength of the X-ray radiation. The average crystallite size obtained for Fe-SoyB was 44.90 nm. The pH_{PZC} value is defined as the pH value at which the negative and positive charges on the adsorbent surface are equal (Kubilay et al., 2007; Nguyen et al., 2024). As show in Fig. 1(f), the pH_{PZC} value of Fe-SoyB was 7.0, comparable to values reported in other studies. For instance, Jiao et al. (2017) reported a pH_{PZC} value of approximately 6.7 for pine sawdust pyrolytic char, while Borba et al. (2019) found a pH_{PZC} value of 6.6 for biochar derived from Pequi (*Caryocar brasiliense*) husks. Additionally, Bagheri et al. (2020) reported a pH_{PZC} value of 7.09 for Moringa seed powder biochar, and Foroutan et al. (2022) found a pH_{PZC} value of 7.6 for hydroxyapatite derived from chicken beak modified with the zeolitic imidazolate framework-8 (ZIF-8).

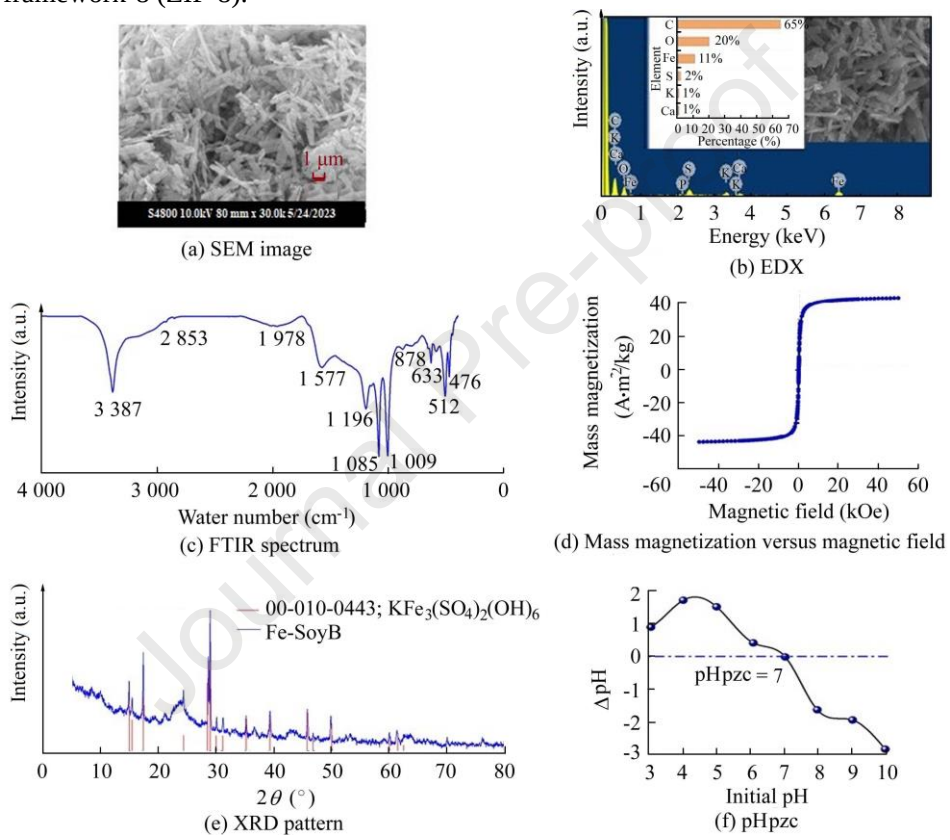

Fig. 1. Characterization of Fe-SoyB.

3.2. Influence of operating parameters on TC degradation

3.2.1. TC removal in different processes

The catalytic efficiency of Fe-SoyB was assessed, and the results are illustrated in Fig. 2. To evaluate the effect of the oxidation process, TC removal was compared in three different systems: Fe-SoyB alone, H_2O_2 alone, and Fe-SoyB combined with H_2O_2 (Fe-SoyB/H_2O_2). The results indicated a significant improvement in TC removal efficiency when H_2O_2 was added. Specifically, the Fe-SoyB/H_2O_2 system achieved nearly 92% degradation of TC after 180 min, whereas only approximately 15% removal was observed in the system with Fe-SoyB alone during the same period. This stark contrast highlighted the effectiveness of the Fe-SoyB/H_2O_2 system in degrading TC. The enhanced removal efficiency can be attributed to the interactions between Fe^{2+} and H_2O_2, which generate

*Corresponding author.
E-mail address: vtdhien@ntt.edu.vn (Thi-Dieu-Hien Vo)

a substantial amount of ·OH, a potent oxidizing agent that plays a crucial role in the degradation process (Lu et al., 1999), thereby facilitating TC removal in the presence of both Fe-SoyB and H_2O_2.

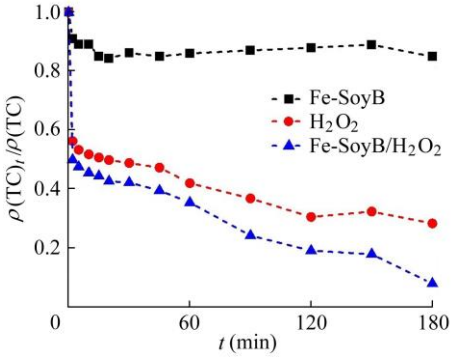

Fig. 2. TC removal in conditions of ρ(TC) = 800 mg/L, c(H_2O_2) = 245 mmol/L, ρ(Fe-SoyB) = 0.5 g/L, pH = 3.0, and T = 25°C (with T denoting reaction temperature and $\rho(TC)_t$ denoting TC concentration at time t).

The synergy factor (F_{syn}) was defined as a function of the reaction rate constants of various processes or mechanisms involved in the Fe-SoyB/H_2O_2 system:

$$F_{syn} = \frac{k_{Fe\text{-}SoyB/H_2O_2}}{k_{Fe\text{-}SoyB} + k_{H_2O_2}} \quad (2)$$

where $k_{Fe\text{-}SoyB/H_2O_2}$, $k_{Fe\text{-}SoyB}$, and $k_{H_2O_2}$ are the reaction rate constants in the Fe-SoyB/H_2O_2, Fe-SoyB, and H_2O_2 systems, respectively. The values of $k_{Fe\text{-}SoyB/H_2O_2}$, $k_{Fe\text{-}SoyB}$, and $k_{H_2O_2}$ were calculated to be 0.143 9 min^{-1}, 0.076 6 min^{-1}, and 0.006 5 min^{-1}, respectively. Using these values, the synergy factor were found to be 1.73. A synergy factor greater than 1.0 indicates a synergistic effect (Moslehi et al., 2024a), suggesting a strong enhancement in the activation of H_2O_2 for improved TC degradation. Additionally, the synergy effect of Fe-SoyB in activating H_2O_2 was calculated using the R factor

$$R = \frac{E_{Fe\text{-}SoyB/H_2O_2}}{E_{Fe\text{-}SoyB} + E_{H_2O_2}} \quad (3)$$

where $E_{Fe\text{-}SoyB/H_2O_2}$, $E_{Fe\text{-}SoyB}$, and $E_{H_2O_2}$ are the TC removal efficiencies of the Fe-SoyB/H_2O_2, Fe-SoyB, and H_2O_2 systems, respectively. The TC removal efficiency of the Fe-SoyB/H_2O_2 system was compared to those of the individual Fe-SoyB and H_2O_2 processes, based on the results presented in Fig. 2. The R factor can be classified into three distinct conditions: (1) antagonism (R < 1), in which the combined effect of individual components is less than the sum of individual effects; (2) additive effect (R = 1), in which the combined effect equals the sum of individual effects, indicating no interaction beyond mere addition; and (3) synergistic effect (R > 1), in which the combined effect exceeds the sum of individual effects, indicating that the components work together to produce a greater effect than expected from their individual contributions (Olfatmehr et al., 2022; Amarzadeh et al., 2023; Moslehi et al., 2024b). Using Eq. (3), an R factor value of 1.06 was obtained for TC degradation using the Fe-SoyB/H_2O_2 system, indicating a good synergistic effect between Fe-SoyB and H_2O_2 in H_2O_2 activation and TC degradation within this system.

3.2.2. Effect of initial pH

The pH value is a critical parameter during the oxidation process (Wang et al., 2016; Li et al., 2022b). The effect of pH on TC degradation in a Fenton-like process using Fe-SoyB as heterogeneous catalyst was investigated. Degradation experiments were conducted at pH values of 3.0, 5.0, 7.0, and 9.0 in the Fe-SoyB/H_2O_2 system. As shown in Fig. 3, TC was efficiently eliminated at pH = 3.0. The result indicated that increasing pH led to a decrease in removal efficiency: from 81.08% (pH = 3.0), to 64.59% (pH = 5.0), 58.12% (pH = 7.0), and finally 51.45% (pH = 9.0). The optimal condition at pH = 3.0 promoted the synthesis of more ·OH, leading to enhanced TC decomposition. This observation aligned with findings from Li et al. (2022a). At high pH values (7−9), the decomposition of H_2O_2 and the reactions between reactive oxygen species predominantly yielded oxygen and hydroperoxyl radicals, which possess lower oxidizing properties than ·OH radicals (Cheng et al., 2023a). Consequently, TC removal was less effective at elevated pH conditions.

*Corresponding author.
E-mail address: vtdhien@ntt.edu.vn (Thi-Dieu-Hien Vo)

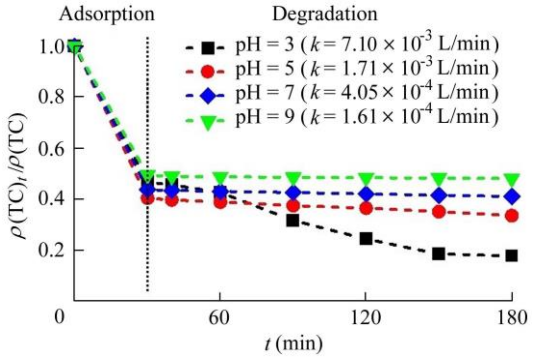

Fig. 3. Impact of initial solution pH on TC degradation (reaction conditions: ρ(TC) = 800 mg/L, ρ(Fe-SoyB) = 0.5 g/L, $c(H_2O_2)$ = 245 mmol/L, and reaction time of 150 min).

In terms of reaction rate, the highest rate constant (k) was calculated to be 7.10×10^{-3} L/min (Fig. 3). This value was considerably lower than those reported for other catalyst materials in the literature (Table 1). Several factors, as listed in Table 1, contributed to the difficulty in making direct comparisons between the rate constant from this study and those from previous studies, particularly the initial TC concentration and the H_2O_2 concentration. In this study, a TC solution at 800 mg/L was utilized, which was approximately six times higher than the concentrations used for other studies listed in Table 1. Additionally, the H_2O_2 dosage was also higher than those of other studies. Although the data indicated that Fe-SoyB had a lower rate constant compared to other catalysts, these variations in experimental conditions necessitate further investigation to confirm the degradation capacity of Fe-SoyB.

Table 1
Rate constants reported in literature.

Catalyst	pH	H_2O_2 concentration (mmol/L)	Initial TC concentration (mg/L)	Catalyst dosage (g/L)	k (L/ min)	Reference
Fe-SoyB	3.0	245	800	0.5	0.007 1	This study
Fe_3O_4-Cs	3.0	10	120	0.5	0.017 0	Li et al. (2020)
Fe_3O_4	3.7	150	100	1.0	0.120 0	Hou et al. (2016)

3.2.3. Effect of H_2O_2 concentration

A study was conducted to investigate the impact of H_2O_2 concentration on the oxidation of TC. The H_2O_2 concentration was systematically varied within the range of 122.5–490.0 mmol/L. As shown in Fig. 4, the rate constant increased from 5.78×10^{-3} L/min to 6.72×10^{-3} L/min with an increase in H_2O_2 concentration. In addition, the TC degradation efficiency increased from approximately 82.0% to 89.5% as the H_2O_2 concentration was increased from 125.5 mmol/L to 367.5 mmol/L. However, further increasing the H_2O_2 concentration to 490 mmol/L did not enhance TC removal beyond this level. This phenomenon can be explained by the consumption of ·OH in the process, which may occur due to the surplus H_2O_2. The reactions can be described by the following equations (Bokare and Choi, 2014; Li et al., 2022b):

$$H_2O_2 + \cdot OH \rightarrow HO_2^{\cdot} + H_2O \quad (4)$$

$$\cdot OH + \cdot OH \rightarrow H_2O_2 \quad (5)$$

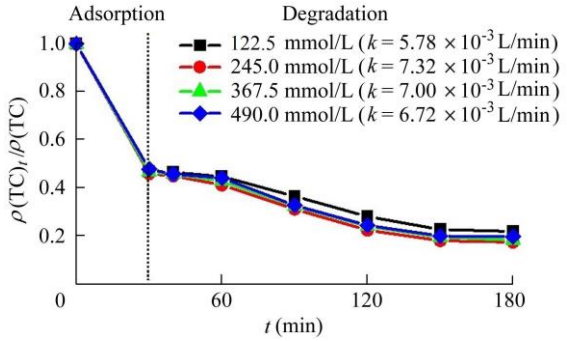

Fig. 4. Impact of H_2O_2 concentration on TC degradation (reaction conditions: ρ(TC) = 800 mg/L, pH = 3.0, ρ(Fe-SoyB) = 0.5 g/L, and reaction time of 150 min).

*Corresponding author.
E-mail address: vtdhien@ntt.edu.vn (Thi-Dieu-Hien Vo)

3.2.4. Effect of initial TC concentration

Another important factor in the elimination of contaminants is the initial TC concentration. As shown in Fig. 5, at an initial TC concentration of 600 mg/L, approximately 72% of TC could be removed within 30 min and 92% in 150 min. As the initial TC concentration was increased to 800 mg/L and 1 000 mg/L, the removal efficiencies correspondingly decreased to 87% and 75%, respectively. This decrease in removal efficiency can be attributed to the constant amount of hydroxyl radicals generated at the same Fe-SoyB catalytic dosage and H_2O_2 concentration. As the TC concentration was increased, the available free radicals became insufficient to effectively break down TC at higher concentrations, resulting in decreased removal efficiency (Li et al., 2022b). Furthermore, the rate constant decreased with increasing initial TC concentration because a low concentration of TC could facilitate a faster oxidation rate. This observation aligned with the findings of Li et al. (2020).

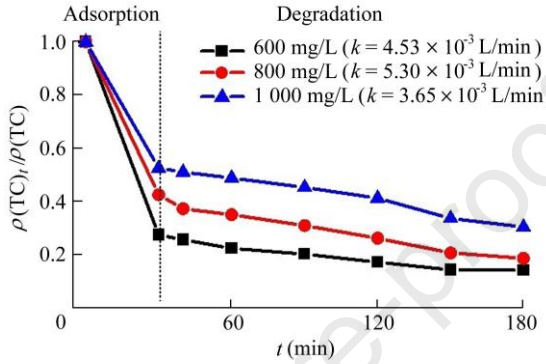

Fig. 5. Impact of initial TC concentration on TC degradation (reaction conditions: ρ(Fe-SoyB) = 0.5 g/L, $c(H_2O_2)$ = 245 mmol/L, and reaction time of 150 min).

3.2.5. Effect of catalyst dosage

As shown in Fig. 6, the efficiency of TC degradation in the Fe-SoyB/H_2O_2 system significantly increased with the rising dosage of Fe-SoyB. The degradation efficiency rose from approximately 61% at an Fe-SoyB dosage of 0.25 g/L to 95% at 0.75 g/L. The rate constant of the Fe-SoyB/H_2O_2 process also exhibited a general upward trend with increasing Fe-SoyB dosage. Specifically, the rate constant value increased from 3.10×10^{-3} L/min at a dosage of 0.25 g/L to 5.19×10^{-3} L/min at 0.75 g/L. These findings indicated that augmenting the dosage of Fe-SoyB enhanced the number of active sites (Liu et al., 2021; Li et al., 2022b).

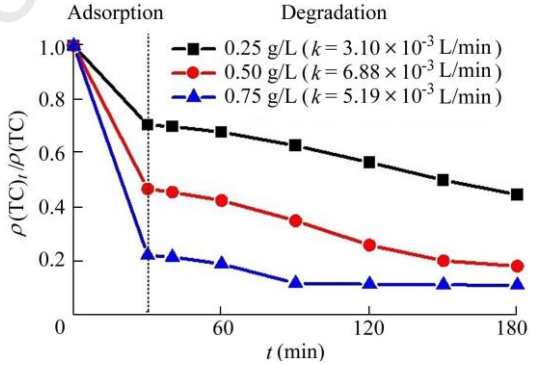

Fig. 6. Impact of catalyst dosage on TC degradation (reaction conditions: ρ(TC) = 800 mg/L, $c(H_2O_2)$ = 245 mmol/L, and reaction time of 150 min).

3.3. Effect of water matrix and reusability of Fe-SoyB for TC degradation

To evaluate TC degradation in the Fe-SoyB system, different real water sources (such as tap water and river water) were used as reaction solvents. The efficiencies of TC degradation were found to be 87.1% in deionized water, 78.5% in tap water, and 72.5% in river water (Fig. 7(a)). Notably, the degradation efficiencies in real water samples were lower than in deionized water, likely due to the presence of competing or quenching chemicals, such as ions and natural organic molecules (Qin et al., 2020). Nevertheless, despite

*Corresponding author.
E-mail address: vtdhien@ntt.edu.vn (Thi-Dieu-Hien Vo)

this disparity, the TC degradation efficiencies in real water samples remained satisfactory (Liu et al., 2021), indicating that the Fe-SoyB/H_2O_2 system shows promise for practical wastewater treatment.

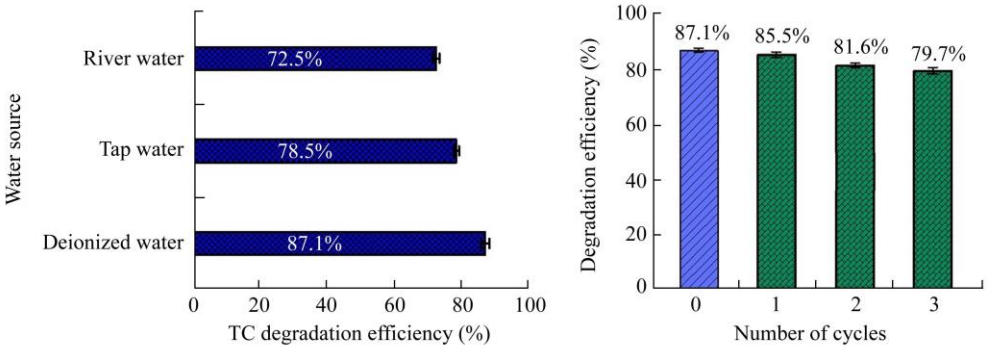

(a) Influence of different water sources on TC degradation in Fe-SoyB/H_2O_2 system

(b) Reusability of Fe-SoyB in H_2O_2 activation for TC degradation

Fig. 7. Influence of different water sources on TC degradation in Fe-SoyB/H_2O_2 system and reusability of Fe-SoyB in H_2O_2 activation for TC degradation (reaction conditions: ρ(Fe-SoyB) = 0.75 g/L, ρ(TC) = 800 mg/L, c(H_2O_2) = 245 mmol/L, and reaction time of 150 min).

The reusability of catalysts is a critical factor for practical application. To verify its reusability performance, the catalyst was first recovered via magnetic separation, washed multiple times with ultrapure water, and then directly introduced into the next cycle. Fig. 7(b) shows that as the number of cycles increased, the removal effectiveness of Fe-SoyB progressively declined. However, the performance of the Fe-SoyB catalyst after the third cycle remained significant, with a marginal drop in efficiency less than 15%, confirming the reusability of Fe-SoyB.

3.4. TC degradation mechanism using Fe-SoyB/H_2O_2

The proposed reaction pathway for TC degradation using Fe-SoyB as a catalyst is schematically shown in Fig. 8. The first stage involves the adsorption of TC onto the surface of the Fe-SoyB catalyst. The rough and porous surface structure of the material facilitates the adsorption process through electrostatic interactions and filling. In addition, the functional groups present on the material's surface promote complexation and ion exchange between TC and the catalyst (Li et al., 2021). In the second stage, α-FeOOH in Fe-SoyB is comprised of Fe^{2+} and Fe^{3+}. Fe^{2+} ions react with H_2O_2 to form ·OH and more Fe^{3+} ions:

$$H_2O_2 + Fe^{2+} \rightarrow \cdot OH + OH^- + Fe^{3+} \quad (6)$$

These ·OH radicals are crucial for the degradation of TC into CO_2, H_2O, and various intermediates. Notably, H_2O_2 can further reduce Fe^{3+} back to Fe^{2+}, allowing the cycle to continue:

$$H_2O_2 + Fe^{3+} \rightarrow HO_2^{\cdot} + H^+ + Fe^{2+} \quad (7)$$

In the Fe-SoyB/H_2O_2 system, ferrous ions are generated according to Eq. (8) (Liou and Lu, 2008):

$$2\alpha\text{-FeOOH} + H_2O_2 + 4H^+ \rightarrow 2Fe^{2+} + O_2 + 4H_2O \quad (8)$$

Hydroxyl radicals may react with ferrous ions to form ferric ions or react with TC (Lu et al., 1999).

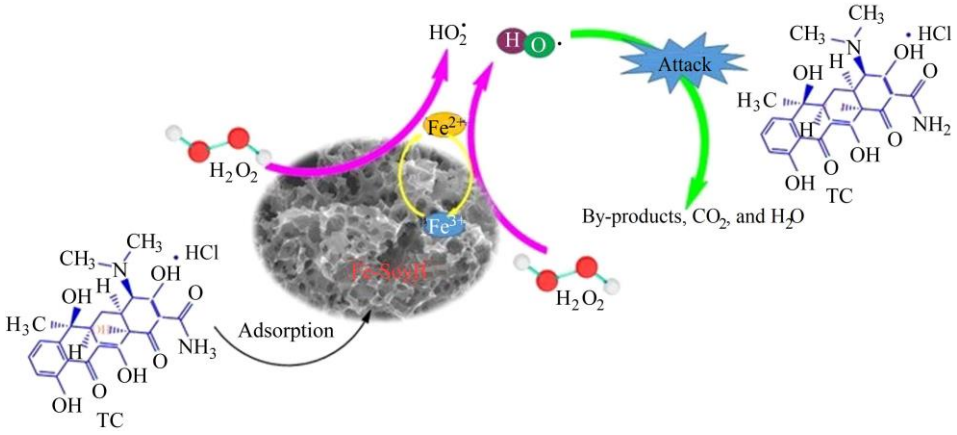

*Corresponding author.
E-mail address: vtdhien@ntt.edu.vn (Thi-Dieu-Hien Vo)

Fig. 8. Proposed reaction pathway for TC degradation in Fe-SoyB/H_2O_2 system.

In addition, the Fe-SoyB/H_2O_2 system was investigated for the formation of ·OH using electron paramagnetic resonance experiments with DMPO. As shown in Fig. 9, noticeable DMPO-OH quartet signals (1:2:2:1) were observed, which were consistent with the hyperfine coupling constants of the DMPO-OH products (Nguyen et al., 2019a; Ma et al., 2020). These findings confirmed that ·OH was the primary radical generated from the catalysis of H_2O_2 by Fe^{2+} in Fe-SoyB. The comparative TC removal efficiencies with various catalysts are presented in Table 2, highlighting the effectiveness of Fe-SoyB in degrading TC compared to other catalytic materials.

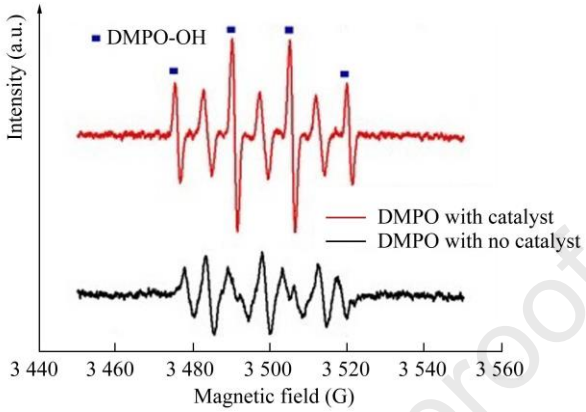

Fig. 9. Electron paramagnetic resonance spectra generated in the presence of DMPO with catalyst and DMPO with no catalyst.

Table 2
Various methods for removing tetracycline.

Reaction system	Reaction conditions	Time (min)	Removal efficiency (%)	References
MCN@CdS/visible light	ρ(TC) = 10 mg/L, catalyst dosage of 0.3 g/L, pH = 4.0, and 300-W Xenon lamp (λ > 420 nm)	120	99.5	Jing et al. (2024)
$MnFe_2O_4$/ZIF 8/xenon	ρ(TC) = 20 mg/L, catalyst dosage of 0.5 g/L, pH = 9.0, and 500-W Xenon lamp (λ = 420 nm)	200	96.1	Azqandi et al. (2024)
FeOCl/NvCN/visible light/H_2O_2	ρ(TC) = 15 mg/L, catalyst dosage of 150 mg/L, c(H_2O_2) = 1 mmol/L, and pH = 4.7	60	95.7	Shao et al. (2024)
Fe^{3+}/H_2O_2	c(TC) = 30 μmol/L, c(Fe^{3+}) = 30 μmol/L, c(H_2O_2) = 4 mmol/L, and pH = 3.0	60	84.5	Liu et al. (2023)
CuS@Cu-CDs/H_2O_2	ρ(TC) = 100 mg/L, catalyst dosage of 0.5 g/L, c(H_2O_2) = 7 mmol/L, and pH = 5.6	30	85.0	Cheng et al. (2023b)
Fe-NCs-1/visible light/H_2O_2	ρ(TC) = 10 mg/L, catalyst dosage of 0.5 g/L, c(H_2O_2) = 10 mmol/L, pH = 5, and temperature of 25°C	90	96.0	Huang et al. (2021)
FeOCl/H_2O_2	ρ(TC) = 60 mg/L, catalyst dosage of 350 mg/L, c(H_2O_2) = 5 mmol/L, and pH= 4	60	92.9	Cao et al. (2021)
$FeNi_3$/SiO_2/H_2O_2	ρ(TC) = 20 mg/L, catalyst dosage of 0.1 g/L, pH = 7, ρ(H_2O_2) = 200 mg/L, and room temperature	180	92.3	Barikbin et al. (2020)
Schorl/H_2O_2	ρ(TC) = 100 mg/L, catalyst dosage of 10.0 g/L, c(H_2O_2) = 9.9 mmol/L, pH = 3.0, and temperature of 40°C	600	95.2	Zhang et al. (2018)
UV/TiO_2/H_2O_2	ρ(TC) = 55 mg/L, ρ(TiO_2) = 1 g/L, ρ(H_2O_2) = 100 mg/L, pH = 5, and 18-W lamp power	30	100	Safari et al. (2015)
Fe-SoyB/H_2O_2	ρ(TC) = 800 mg/L, catalyst dosage of 0.75 g/L, c(H_2O_2) = 245 mmol/L, pH = 3, and temperature of 25°C	150	90.0	This study

4. Conclusions

In this study, Fe-SoyB was used as an excellent heterogeneous Fenton catalyst for effectively degrading TC. The biochar exhibited satisfactory catalytic performance and structural stability, with the TC degradation efficiency in the Fe-SoyB/H_2O_2 system influenced by various factors, including catalyst dosage, initial pH, H_2O_2 concentration, and initial TC concentration. Under optimal conditions (an initial pH of 3.0, an H_2O_2 concentration of 245 mmol/L, an initial TC concentration of 800 mg/L, and a catalyst dosage of 0.75 g/L), the removal efficiency reached up to 90%. The quenching tests confirmed that ·OH was the primary oxidant responsible for TC degradation in the Fe-SoyB/H_2O_2 system. Given its strong reusability and catalytic performance, the Fe-SoyB/H_2O_2 system shows significant potential for removing TC from wastewater. Therefore, further extensive and practical investigations are required to assess the system's applicability in real-world wastewater treatment scenarios. This study demonstrated that the Fe-SoyB biochar is an environmentally friendly, economically viable, and technically effective absorbent. Future research should explore its efficacy

*Corresponding author.
E-mail address: vtdhien@ntt.edu.vn (Thi-Dieu-Hien Vo)

in removing other emerging pollutants, such antibiotics, pesticides, endocrine disruptors, and personal care items, which have garnered significant attention in recent years.

Acknowledgments

The authors wish to express their gratitude for the collaborative efforts of researchers from various universities. We would especially like to thank Mr. Thanh-Trung-Ninh Pham and Miss Thi-Ngoc-Tuyen Le for their invaluable assistance with sample collection throughout the study.

Declaration of competing interest

The authors declare no conflicts of interest.

References

Akindolie, M.S., Choi, H.J., 2022. Surface modification of spent coffee grounds using phosphoric acid for enhancement of methylene blue adsorption from aqueous solution. Water Sci. Technol. 85(4), 1218–1234. https://doi.org/10.2166/wst.2022.021.

Amarzadeh, M., Azqandi, M., Nateq, K., Ramavandi, B., Khan, N.A., Nasseh, N., 2023. Heterogeneous Fenton-like photocatalytic process towards the eradication of tetracycline under UV irradiation: Mechanism elucidation and environmental risk analysis. Water 15(3), 2336. https://doi.org/10.3390/w15132336.

Azqandi, M., Nateq, K., Amarzadeh, M., Yoosefian, M., Yaghoot-Nezhad, A., Ahmad, A., Ramavandi, B., Nasseh, N., 2024. Intensified photo-decontamination of tetracycline antibiotic by S-scheme spinel manganese ferrite-grafted ZIF-8 heterojunction photocatalyst: Mechanism conception, degradation pathway and DFT studies. Journal of Environmental Chemical Engineering 12(3), 112875. https://doi.org/10.1016/j.jece.2024.112875.

Bagheri, A., Abu-Danso, E., Iqbal, J., Bhatnagar, A., 2020. Modified biochar from Moringa seed powder for the removal of diclofenac from aqueous solution. Environmental Science and Pollution Research 27(7), 7318–7327. https://doi.org/10.1007/s11356-019-06844-x.

Baird, R., Rice, E., Eaton, A., 2017. Standard Methods for the Examination of Water and Wastewaters. American Water Works Association, Denver.

Barikbin, B., Arghavan, F.S., Othmani, A., Panahi, A.H., Nasseh, N., 2020. Degradation of tetracycline in Fenton and heterogeneous Fenton like processes by using $FeNi_3$ and $FeNi_3/SiO_2$ catalysts. Desalin. Water Treat. 200, 262–274. https://doi.org/10.5004/dwt.2020.26061.

Bokare, A.D., Choi, W., 2014. Review of iron-free Fenton-like systems for activating H_2O_2 in advanced oxidation processes. J. Hazard. Mater. 275, 121–135. https://doi.org/10.1016/j.jhazmat.2014.04.054.

Borba, L.L., Cuba, R.M.F., Terán, F.J.C., Castro, M.N., Mendes, T.A., 2019. Use of adsorbent biochar from pequi (*Caryocar brasiliense*) husks for the removal of commercial formulation of glyphosate from aqueous media. Brazilian Archives of Biology and Technology 62(10), e19180450. https://doi.org/10.1590/1678-4324-2019180450.

Cao, Y., Cui, K., Chen, Y., Cui, M., Li, G., Li, D., Yang, X., 2021. Efficient degradation of tetracycline by H_2O_2 catalyzed by FeOCl: A wide range of pH values from 3 to 7. Solid State Sci. 113, 106548. https://doi.org/10.1016/j.solidstatesciences.2021.106548.

Chen, L., Mi, B., He, J., Li, Y., Zhou, Z., Wu, F., 2023. Functionalized biochars with highly-efficient malachite green adsorption property produced from banana peels via microwave-assisted pyrolysis. Bioresour. Technol. 376, 128840. https://doi.org/10.1016/j.biortech.2023.128840.

Cheng, X., Liang, L., Ye, J., Li, N., Yan, B., Chen, G., 2023a. Influence and mechanism of water matrices on H_2O_2-based Fenton-like oxidation processes: A review. Sci. Total Environ. 888, 164086. https://doi.org/10.1016/j.scitotenv.2023.164086.

Cheng, Y., Deng, L., Wang, D., Wang, X., Ji, C., Zhou, Y.H., 2023b. CuS@ Cu-CD composites as efficient heterogeneous Fenton-like catalysts for the photodegradation of tetracycline. Adv. Environ. Sci. 2(3), 495–507. https://doi.org/10.1039/d2va00139j.

Cho, D.W., Yoon, K., Kwon, E.E., Biswas, J.K., Song, H., 2017. Fabrication of magnetic biochar as a treatment medium for As(V) via pyrolysis of $FeCl_3$-pretreated spent coffee ground. Environ. Pollut. 229, 942–949. https://doi.org/10.1016/j.envpol.2017.07.079.

Devi, P., Saroha, A.K., 2017. Utilization of sludge based adsorbents for the removal of various pollutants: A review. Sci. Total Environ. 578, 16–33. https://doi.org/10.1016/j.scitotenv.2016.10.220.

Du, L., Ahmad, S., Liu, L., Wang, L., Tang, J., 2023. A review of antibiotics and antibiotic resistance genes (ARGs) adsorption by biochar and modified biochar in water. Sci. Total Environ. 858, 159815. https://doi.org/10.1016/j.scitotenv.2022.159815.

Foroutan, R., Jamaleddin Peighambardoust, S., Amarzadeh, M., Kiani Korri, A., Sadat Peighambardoust, N., Ahmad, A., Ramavandi, B., 2022. Nickel ions abatement from aqueous solutions and shipbuilding industry wastewater using ZIF-8-chicken beak hydroxyapatite. Journal of Molecular Liquids 356, 119003. https://doi.org/10.1016/j.molliq.2022.119003.

Fu, M.M., Mo, C.H., Li, H., Zhang, Y.N., Huang, W.X., Wong, M.H., 2019. Comparison of physicochemical properties of biochars and hydrochars produced from food wastes. Journal of Cleaner Production 236, 117637. https://doi.org/10.1016/j.jclepro.2019.117637.

Ganesapillai, M., Mehta, R., Tiwari, A., Sinha, A., Bakshi, H.S., Chellappa, V., Drewnowski, J., 2023. Waste to energy: A review of biochar production with emphasis on mathematical modelling and its applications. Heliyon 9(4), e14873. https://doi.org/10.1016/j.heliyon.2023.e14873.

*Corresponding author.
E-mail address: vtdhien@ntt.edu.vn (Thi-Dieu-Hien Vo)

Ghanbari, F., Riahi, M., Kakavandi, B., Hong, X., Lin, K.Y.A., 2020. Intensified peroxydisulfate/microparticles-zero valent iron process through aeration for degradation of organic pollutants: Kinetic studies, mechanism and effect of anions. Journal of Water Process Engineering 36, 101321. https://doi.org/10.1016/j.jwpe.2020.101321.

Hou, L., Wang, L., Royer, S., Zhang, H., 2016. Ultrasound-assisted heterogeneous Fenton-like degradation of tetracycline over a magnetite catalyst. J. Hazard. Mater. 302, 458–467. https://doi.org/10.1016/j.jhazmat.2015.09.033.

Hu, T., Zhao, S., Huang, Y., Chen, Z., Zhang, X., Wei, C., Zeng, S., Liu, L., 2023. Potential removals of tetracycline and sulfamethoxazole by iron-loaded sludge biochar. J. Water Process. Eng. 54, 103962. https://doi.org/10.1016/j.jwpe.2023.103962.

Huang, X., Zhou, H., Yue, X., Ran, S., Zhu, J., 2021. Novel magnetic Fe_3O_4/α-FeOOH nanocomposites and their enhanced mechanism for tetracycline hydrochloride removal in the visible photo-Fenton process. ACS Omega 6(13), 9095–9103. https://doi.org/10.1021/acsomega.1c00204.

Huang, Z., Fang, X., Wang, S., Zhou, N., Fan, S., 2023. Effects of $KMnO_4$ pre- and post-treatments on biochar properties and its adsorption of tetracycline. J. Mol. Liq. 373, 121257. https://doi.org/10.1016/j.molliq.2023.121257.

Isaac, R., Siddiqui, S., Aldosari, O.F., Kashif Uddin, M., 2023. Magnetic biochar derived from *Juglans regia* for the adsorption of Cu^{2+} and Ni^{2+}: Characterization, modelling, optimization, and cost analysis. J. Saudi Chem. Soc. 27(6), 101749. https://doi.org/10.1016/j.jscs.2023.101749.

Jaiswal, A., Banerjee, S., Mani, R., Chattopadhyaya, M.C., 2013. Synthesis, characterization and application of goethite mineral as an adsorbent. J. Environ. Chem. Eng. 1(3), 281–289. https://doi.org/10.1016/j.jece.2013.05.007.

Jaiswal, K.K., Kumar, V., Vlaskin, M.S., Nanda, M., Verma, M., Ahmad, W., Kim, H., 2021. Hydropyrolysis of freshwater macroalgal bloom for bio-oil and biochar production: Kinetics and isotherm for removal of multiple heavy metals. Environ. Technol. Innov. 22, 101440. https://doi.org/10.1016/j.eti.2021.101440.

Jang, H.M., Kan, E., 2019. A novel hay-derived biochar for removal of tetracyclines in water. Bioresource Technology 274, 162–172. https://doi.org/10.1016/j.biortech.2018.11.081.

Jiang, H., Dai, Y., 2023. Vitamin C modified crayfish shells biochar efficiently remove tetracycline from water: A good medicine for water restoration. Chemosphere 311, 136884. https://doi.org/10.1016/j.chemosphere.2022.136884.

Jiang, W., Cai, Y., Liu, D., Shi, Q., Wang, Q., 2023. Adsorption properties and mechanism of suaeda biochar and modified materials for tetracycline. Environ. Res. 235, 116549. https://doi.org/10.1016/j.envres.2023.116549.

Jiao, Y., Han, D., Lu, Y., Rong, Y., Fang, L., Liu, Y., Han, R., 2017. Characterization of pine-sawdust pyrolytic char activated by phosphoric acid through microwave irradiation and adsorption property toward CDNB in batch mode. Desalination and Water Treatment 77, 247–255. https://doi.org/10.5004/dwt.2017.20780.

Jing, S., Zhao, J., Wang, A., Ji, Q., Cheng, R., Liang, H., Chen, F., Kannan, P., Brouzgou, A., Tsiakaras, P., 2024. Efficient photocatalytic production of H_2O_2 and photodegradation of tetracycline by CdS/square tubular g-C_3N_4 S-scheme heterojunction photocatalyst. Chemical Engineering Journal 479, 147150. https://doi.org/10.1016/j.cej.2023.147150.

Kakavandi, B., Babaei, A.A., 2016. Heterogeneous Fenton-like oxidation of petrochemical wastewater using a magnetically separable catalyst (MNPs@C): Process optimization, reaction kinetics and degradation mechanisms. RSC Advances 6(88), 84999–85011. https://doi.org/10.1039/C6RA17624K.

Kubilay, Ş., Gürkan, R., Savran, A., Şahan, T., 2007. Removal of Cu(II), Zn(II) and Co(II) ions from aqueous solutions by adsorption onto natural bentonite. Adsorption 13(1), 41–51. https://doi.org/10.1007/s10450-007-9003-y.

Kurniawan, T.A., Othman, M.H.D., Liang, X., Goh, H.H., Gikas, P., Chong, K.K., Chew, K.W., 2023. Challenges and opportunities for biochar to promote circular economy and carbon neutrality. J. Environ. Manage. 332, 117429. https://doi.org/10.1016/j.jenvman.2023.117429.

Lee, Y.J., Lee, J.M., Huang, M., Park, S.J., Lee, C.G., 2023. Degradation of imidacloprid via the activation of peroxymonosulfate and peroxydisulfate using a Fenton-sludge-derived Fe^0/Fe_3C composite. J. Water Process. Eng. 56, 104347. https://doi.org/10.1016/j.jwpe.2023.104347.

Li, D., Yu, J., Jia, J., He, H., Shi, W., Zheng, T., Ma, J., 2022a. Coupling electrode aeration and hydroxylamine for the enhanced electro-Fenton degradation of organic contaminant: Improving H_2O_2 generation, Fe^{3+}/Fe^{2+} cycle and N_2 selectivity. Water Res. 214, 118167. https://doi.org/10.1016/j.watres.2022.118167.

Li, J., Liu, Y., Ren, X., Dong, W., Chen, H., Cai, T., Zeng, W., Li, W., Tang, L., 2021. Soybean residue based biochar prepared by ball milling assisted alkali activation to activate peroxydisulfate for the degradation of tetracycline. J. Colloid Interface Sci. 599, 631–641. https://doi.org/10.1016/j.jcis.2021.04.074.

Li, S., Han, K., Li, J., Li, M., Lu, C., 2017. Preparation and characterization of super activated carbon produced from gulfweed by KOH activation. Micropor. Mesopor. Mat. 243, 291–300. https://doi.org/10.1016/j.micromeso.2017.02.052.

Li, X., Cui, K., Guo, Z., Yang, T., Cao, Y., Xiang, Y., Chen, H., Xi, M., 2020. Heterogeneous Fenton-like degradation of tetracyclines using porous magnetic chitosan microspheres as an efficient catalyst compared with two preparation methods. Chem. Eng. J. 379, 122324. https://doi.org/10.1016/j.cej.2019.122324.

Li, X., Jia, Y., Zhang, J., Qin, Y., Wu, Y., Zhou, M., Sun, J., 2022b. Efficient removal of tetracycline by H_2O_2 activated with iron-doped biochar: Performance, mechanism, and degradation pathways. Chin. Chem. Lett. 33(4), 2105–2110. https://doi.org/10.1016/j.cclet.2021.08.054.

Li, Y., Gupta, R., Zhang, Q., You, S., 2023. Review of biochar production via crop residue pyrolysis: Development and perspectives. Bioresour. Technol. 369, 128423. https://doi.org/10.1016/j.biortech.2022.128423.

Liou, M.J., Lu, M.C., 2008. Catalytic degradation of explosives with goethite and hydrogen peroxide. J. Hazard. Mater. 151(2), 540–546. https://doi.org/10.1016/j.jhazmat.2007.06.016.

*Corresponding author.
E-mail address: vtdhien@ntt.edu.vn (Thi-Dieu-Hien Vo)

Liu, J., Li, X., Chu, Y., Yuan, L., Lv, R., Zhang, W., 2023. An autocatalytic Fe(III)/H_2O_2 Fenton-like process triggered by tetracycline: The overlooked effect of quinone intermediates. Chem. Eng. J. 475, 146035. https://doi.org/10.1016/j.cej.2023.146035.

Liu, P., Li, H., Liu, X., Wan, Y., Han, X., Zou, W., 2020. Preparation of magnetic biochar obtained from one-step pyrolysis of *Salix mongolica* and investigation into adsorption behavior of sulfadimidine sodium and norfloxacin in aqueous solution. J. Dispers. Sci. Technol. 41(2), 214–226. https://doi.org/10.1080/01932691.2018.1562354.

Liu, Q., Zheng, Y., Zhong, L., Cheng, X., 2015. Removal of tetracycline from aqueous solution by a Fe_3O_4 incorporated PAN electrospun nanofiber mat. Journal of Environmental Sciences 28, 29–36. https://doi.org/10.1016/j.jes.2014.04.016.

Liu, Y., Li, J., Wu, L., Wan, D., Shi, Y., He, Q., Chen, J., 2021. Synergetic adsorption and Fenton-like degradation of tetracycline hydrochloride by magnetic spent bleaching earth carbon: Insights into performance and reaction mechanism. Sci. Total Environ. 761, 143956. https://doi.org/10.1016/j.scitotenv.2020.143956.

Lu, M.C., Chen, J.N., Chang, C.P., 1999. Oxidation of dichlorvos with hydrogen peroxide using ferrous ion as catalyst. J. Hazard. Mater. 65(3), 277–288. https://doi.org/10.1016/S0304-3894(98)00268-4.

Luo, Y., Zheng, A., Li, J., Han, Y., Xue, M., Zhang, L., Yin, Z., Xie, C., Chen, Z., Ji, L., et al., 2023. Integrated adsorption and photodegradation of tetracycline by bismuth oxycarbonate/biochar nanocomposites. Chem. Eng. J. 457, 141228. https://doi.org/10.1016/j.cej.2022.141228.

Ma, C., Jia, S., Yuan, P., He, Z., 2020. Catalytic ozonation of 2,2′-methylenebis (4-methyl-6-tert-butylphenol) over nano-Fe_3O_4@cow dung ash composites: Optimization, toxicity, and degradation mechanisms. Environ. Pollut. 265, 114597. https://doi.org/10.1016/j.envpol.2020.114597.

Markovski, J.S., Đokić, V., Milosavljević, M., Mitrić, M., Perić-Grujić, A.A., Onjia, A.E., Marinković, A.D., 2014. Ultrasonic assisted arsenate adsorption on solvothermally synthesized calcite modified by goethite, α-MnO_2 and goethite/α-MnO_2. Ultrason. Sonochem. 21(2), 790–801. https://doi.org/10.1016/j.ultsonch.2013.10.006.

Massoudi, J., Smari, M., Nouri, K., Dhahri, E., Khirouni, K., Bertaina, S., Bessais, L., Hlil, E.K., 2020. Magnetic and spectroscopic properties of Ni–Zn–Al ferrite spinel: From the nanoscale to microscale. RSC Advances 10(57), 34556–34580. https://doi.org/10.1039/D0RA05522K.

Mateos-Aparicio, I., Mateos-Peinado, C., Rupérez, P., 2010. High hydrostatic pressure improves the functionality of dietary fibre in okara by-product from soybean. Innov. Food Sci. Emerg. Technol. 11(3), 445–450. https://doi.org/10.1016/j.ifset.2010.02.003.

Moslehi, M.H., Eslami, M., Ghadirian, M., Nateq, K., Ramavandi, B., Nasseh, N., 2024a. Photocatalytic decomposition of metronidazole by zinc hexaferrite coated with bismuth oxyiodide magnetic nanocomposite: Advanced modelling and optimization with artificial neural network. Chemosphere 356, 141770. https://doi.org/10.1016/j.chemosphere.2024.141770.

Moslehi, M.H., Zadeh, M.S., Nateq, K., Shahamat, Y.D., Khan, N.A., Nasseh, N., 2024b. Statistical computational optimization approach for photocatalytic-ozonation decontamination of metronidazole in aqueous media using $CuFe_2O_4/SiO_2$/ZnO nanocomposite. Environmental Research 242, 117747. https://doi.org/10.1016/j.envres.2023.117747.

Nguyen, T.B., Huang, C.P., Doong, R., 2019a. Photocatalytic degradation of bisphenol A over a $ZnFe_2O_4/TiO_2$ nanocomposite under visible light. Sci. Total Environ. 646, 745–756. https://doi.org/10.1016/j.scitotenv.2018.07.352.

Nguyen, T.B., Nguyen, T.K.T., Chen, W.H., Chen, C.W., Bui, X.T., Patel, A.K., Dong, C.D., 2023. Hydrothermal and pyrolytic conversion of sunflower seed husk into novel porous biochar for efficient adsorption of tetracycline. Bioresour. Technol. 373, 128711. https://doi.org/10.1016/j.biortech.2023.128711.

Nguyen, T.T., Bui, X.T., Dang, B.T., Ngo, H.H., Jahng, D., Fujioka, T., Chen, S.S., Dinh, Q.T., Nguyen, C.N., Nguyen, P.T.V., 2019b. Effect of ciprofloxacin dosages on the performance of sponge membrane bioreactor treating hospital wastewater. Bioresour. Technol. 273, 573–580. https://doi.org/10.1016/j.biortech.2018.11.058.

Nguyen, V.T., Nguyen, T.B., Huang, C.P., Chen, C.W., Bui, X.T., Dong, C.D., 2021. Alkaline modified biochar derived from spent coffee ground for removal of tetracycline from aqueous solutions. J. Water Process. Eng. 40, 101908. https://doi.org/10.1016/j.jwpe.2020.101908.

Nguyen, V.T., Nguyen, T.B., Vo, T.D.H., Dat, N.D., Vo, T.K.Q., Nguyen, X.C., Dinh, V.C., Le, T.N.C., Duong, T.G.H., Bui, M.H., et al., 2024. Preliminary study of doxycycline adsorption from aqueous solution on alkaline modified biochar derived from banana peel. Environmental Engineering Research 29(3), 230196. https://doi.org/10.4491/eer.2023.196.

Nidheesh, P.V., 2015. Heterogeneous Fenton catalysts for the abatement of organic pollutants from aqueous solution: A review. RSC Advances 5(51), 40552–40577. https://doi.org/10.1039/C5RA02023A.

Nikzad, M., Mousavi, S.Y., Heydarian, M., Rahmani, S., Shabanian, S.R., Hejazi, F., 2024. A review on recent advances in photodegradation of tetracycline in aqueous media. Journal of the Iranian Chemical Society 21(4), 887–902. https://doi.org/10.1007/s13738-024-02982-3.

Olfatmehr, N., Kakavandi, B., Khezri, S.M., 2022. Peroxydisulfate activation by enhanced catalytic activity of $CoFe_2O_4$ anchored on activated carbon: A new sulfate radical-based oxidation study on the cefixime degradation. Separation and Purification Technology 302, 121991. https://doi.org/10.1016/j.seppur.2022.121991.

Ortiz-Ramos, U., Leyva-Ramos, R., Mendoza-Mendoza, E., Aragón-Piña, A., 2022. Removal of tetracycline from aqueous solutions by adsorption on raw Ca-bentonite. Effect of operating conditions and adsorption mechanism. Chemical Engineering Journal 432, 134428. https://doi.org/10.1016/j.cej.2021.134428.

Peng, Z., Li, S., He, H., Wen, Y., Huang, H., Su, L., Yi, Z., Peng, X., Zhou, N., 2023. FeS and Fe_3O_4 Co-modified biochar to build a highly resistant advanced oxidation process system for quinclorac degradation in irrigation water. J. Environ. Manage. 348, 119492. https://doi.org/10.1016/j.jenvman.2023.119492.

*Corresponding author.

E-mail address: vtdhien@ntt.edu.vn (Thi-Dieu-Hien Vo)

Qin, H., Cheng, H., Li, H., Wang, Y., 2020. Degradation of ofloxacin, amoxicillin and tetracycline antibiotics using magnetic core–shell $MnFe_2O_4$@C-NH_2 as a heterogeneous Fenton catalyst. Chem. Eng. J. 396, 125304. https://doi.org/10.1016/j.cej.2020.125304.

Qin, X., Cheng, S., Xing, B., Xiong, C., Yi, G., Shi, C., Xia, H., Zhang, C., 2023. Preparation of high-efficient $MgCl_2$ modified biochar toward Cd(II) and tetracycline removal from wastewater. Sep. Purif. Technol. 325, 124625. https://doi.org/10.1016/j.seppur.2023.124625.

Safari, G.H., Hoseini, M., Seyedsalehi, M., Kamani, H., Jaafari, J., Mahvi, A.H., 2015. Photocatalytic degradation of tetracycline using nanosized titanium dioxide in aqueous solution. Int. J. Environ. Sci. Technol. 12(2), 603–616. https://doi.org/10.1007/s13762-014-0706-9.

Santhosh, C., Daneshvar, E., Tripathi, K.M., Baltrėnas, P., Kim, T., Baltrėnaitė, E., Bhatnagar, A., 2020. Synthesis and characterization of magnetic biochar adsorbents for the removal of Cr(VI) and acid orange 7 dye from aqueous solution. Environmental Science and Pollution Research 27(26), 32874–32887. https://doi.org/10.1007/s11356-020-09275-1.

Sevilla, M., Fuertes, A.B., 2009. Chemical and structural properties of carbonaceous products obtained by hydrothermal carbonization of saccharides. Chem. Eur. J. 15(16), 4195–4203. https://doi.org/10.1002/chem.200802097.

Shao, C., Zhang, J., Wang, Z., Zhang, L., Wang, B., Ren, J., Zhang, X., He, W., 2024. Photo-Fenton degradation of tetracycline on nitrogen vacancy and potassium-doped Z-scheme FeOCl/NvCN heterojunction with low H_2O_2 consumption: Activity and mechanism. Journal of Alloys and Compounds 970, 172532. https://doi.org/10.1016/j.jallcom.2023.172532.

Shi, Q., Wang, W., Zhang, H., Bai, H., Liu, K., Zhang, J., Li, Z., Zhu, W., 2023. Porous biochar derived from walnut shell as an efficient adsorbent for tetracycline removal. Bioresour. Technol. 383, 129213. https://doi.org/10.1016/j.biortech.2023.129213.

Son, E.B., Poo, K.M., Chang, J.S., Chae, K.J., 2018. Heavy metal removal from aqueous solutions using engineered magnetic biochars derived from waste marine macro-algal biomass. Sci. Total Environ. 615, 161–168. https://doi.org/10.1016/j.scitotenv.2017.09.171.

Su, R., Chai, L., Tang, C., Li, B., Yang, Z., 2018. Comparison of the degradation of molecular and ionic ibuprofen in a UV/H_2O_2 system. Water Sci. Technol. 77(9), 2174–2183. https://doi.org/10.2166/wst.2018.129.

Su, R., Dai, X., Wang, H., Wang, Z., Li, Z., Chen, Y., Luo, Y., Ouyang, D., 2022. Metronidazole degradation by UV and UV/H_2O_2 advanced oxidation processes: Kinetics, mechanisms, and effects of natural water matrices. Int. J. Env. Res. Public Health 19(19), 12354. https://doi.org/10.3390/ijerph191912354.

Sun, J., Zhu, W., Cao, J., Zhong, J., Mu, B., Wang, X., Lin, N., 2023a. Improving the yield and tetracycline adsorption performance of kitchen waste biochar through subcritical dimethyl ether pretreatment. J. Environ. Chem. Eng. 11(5), 110459. https://doi.org/10.1016/j.jece.2023.110459.

Sun, K., Jin, J., Keiluweit, M., Kleber, M., Wang, Z., Pan, Z., Xing, B., 2012. Polar and aliphatic domains regulate sorption of phthalic acid esters (PAEs) to biochars. Bioresour. Technol. 118, 120–127. https://doi.org/10.1016/j.biortech.2012.05.008.

Sun, M., Ma, Y., Yang, Y., Zhu, X., 2023b. Effect of iron impregnation ratio on the properties and adsorption of KOH activated biochar for removal of tetracycline and heavy metals. Bioresour. Technol. 380, 129081. https://doi.org/10.1016/j.biortech.2023.129081.

Sun, Y., Li, C., Zhang, S., Li, Q., Gholizadeh, M., Wang, Y., Hu, S., Xiang, J., Hu, X., 2021. Pyrolysis of soybean residue: Understanding characteristics of the products. Renewable Energy 174, 487–500. https://doi.org/10.1016/j.renene.2021.04.063.

Tang, J., Ma, Y., Zeng, C., Yang, L., Cui, S., Zhi, S., Yang, F., Ding, Y., Zhang, K., Zhang, Z., 2023. Fe-Al bimetallic oxides functionalized-biochar via ball milling for enhanced adsorption of tetracycline in water. Bioresour. Technol. 369, 128385. https://doi.org/10.1016/j.biortech.2022.128385.

United States Department of Agriculture (USDA), 2024. World Agricultural Supply and Demand Estimates. USDA, Washington D.C.

Wang, B., Jiang, Y.S., Li, F.Y., Yang, D.Y., 2017. Preparation of biochar by simultaneous carbonization, magnetization and activation for norfloxacin removal in water. Bioresour. Technol. 233, 159–165. https://doi.org/10.1016/j.biortech.2017.02.103.

Wang, N., Zheng, T., Zhang, G., Wang, P., 2016. A review on Fenton-like processes for organic wastewater treatment. J. Environ. Chem. Eng. 4(1), 762–787. https://doi.org/10.1016/j.jece.2015.12.016.

Weidner, E., Siwińska-Ciesielczyk, K., Moszyński, D., Jesionowski, T., Ciesielczyk, F., 2021. A comprehensive method for tetracycline removal using lanthanum-enriched titania–zirconia oxide system with tailored physicochemical properties. Environ. Technol. Innov. 24, 102016. https://doi.org/10.1016/j.eti.2021.102016.

Wijitkosum, S., 2022. Biochar derived from agricultural wastes and wood residues for sustainable agricultural and environmental applications. Int. Soil Water Conserv. Res. 10(2), 335–341. https://doi.org/10.1016/j.iswcr.2021.09.006.

Yang, X., Fan, J., Jiang, L., Zhu, F., Yan, Z., Li, X., Jiang, P., Li, X., Xue, S., 2024. Using Fe/H_2O_2-modified biochar to realize field-scale Sb/As stabilization and soil structure improvement in an Sb smelting site. Sci. Total Environ. 912, 168775. https://doi.org/10.1016/j.scitotenv.2023.168775.

Zhang, H., Wan, K., Yan, J., Li, Q., Guo, Y., Huang, L., Arulmani, S.R.B., Luo, J., 2024. The function of doping nitrogen on removing fluoride with decomposing La-MOF-NH_2: Density functional theory calculation and experiments. J. Environ. Sci. 135, 118–129. https://doi.org/10.1016/j.jes.2023.01.015.

Zhang, X., Zhen, D., Liu, F., Chen, R., Peng, Q., Wang, Z., 2023a. An achieved strategy for magnetic biochar for removal of tetracyclines and fluoroquinolones: Adsorption and mechanism studies. Bioresour. Technol. 369, 128440. https://doi.org/10.1016/j.biortech.2022.128440.

Zhang, Y., Shi, J., Xu, Z., Chen, Y., Song, D., 2018. Degradation of tetracycline in a schorl/H_2O_2 system: Proposed mechanism and intermediates. Chemosphere 202, 661–668. https://doi.org/10.1016/j.chemosphere.2018.03.116.

Zhang, Y., Zhang, J., Chen, K., Shen, S., Hu, H., Chang, M., Chen, D., Wu, Y., Yuan, H., Wang, Y., 2023b. Engineering banana-peel-derived biochar for the rapid adsorption of tetracycline based on double chemical activation. Resour. Conserv. Recy. 190, 106821. https://doi.org/10.1016/j.resconrec.2022.106821.

*Corresponding author.

E-mail address: vtdhien@ntt.edu.vn (Thi-Dieu-Hien Vo)

Zhao, L., Zhao, Y.G., Jin, C., Yang, D., Zhang, Y., Progress, M., 2024. Removal of tetracycline by ultraviolet/sodium percarbonate (UV/SPC) advanced oxidation process in water. Environmental Research 247, 118260. https://doi.org/10.1016/j.envres.2024.118260.

Zhao, W., Chen, L., Jiang, Y., 2023. Preparation of activated carbon from sunflower straw through H_3PO_4 activation and its application for acid fuchsin dye adsorption. Water Sci. Eng. 16(2), 192–202. https://doi.org/10.1016/j.wse.2023.02.002.

Zhu, X., Liu, Y., Qian, F., Zhou, C., Zhang, S., Chen, J., 2014. Preparation of magnetic porous carbon from waste hydrochar by simultaneous activation and magnetization for tetracycline removal. Bioresour. Technol. 154, 209–214. https://doi.org/10.1016/j.biortech.2013.12.019.

Zhu, Y.G., Johnson, T.A., Su, J.Q., Qiao, M., Guo, G.X., Stedtfeld, R.D., Hashsham, S.A., Tiedje, J.M., 2013. Diverse and abundant antibiotic resistance genes in Chinese swine farms. Proceedings of the National Academy of Sciences of the United States of America 110(9), 3435–3440. 10.1073/pnas.1222743110.

*Corresponding author.
E-mail address: vtdhien@ntt.edu.vn (Thi-Dieu-Hien Vo)